Archival Report

Biological Psychiatry: CNNI

Gamma Band Phase Delay in Schizophrenia

Brian J. Roach, Judith M. Ford, and Daniel H. Mathalon

ABSTRACT

BACKGROUND: In 1999, Kwon *et al.* reported several electroencephalographic gamma band auditory steady-state response (ASSR) abnormalities in schizophrenia, spawning approximately 100 subsequent studies. While many studies replicated the finding of reduced 40-Hz ASSR power in schizophrenia and extended this by showing that 40-Hz phase synchrony (phase-locking factor [PLF]) was also reduced, none attempted to replicate the original phase delay finding of Kwon *et al.* Accordingly, we measured the 40-Hz ASSR phase-locking angle (PLA) to assess phase delay and examined its differential sensitivity to schizophrenia, relative to power and PLF measures.

METHODS: To obtain ASSRs, electroencephalography data were recorded from 28 patients with schizophrenia and 25 healthy control subjects listening to repeated 40-Hz 500-ms click trains. Evoked power, total power, PLF, and PLA were calculated after Morlet wavelet time-frequency decomposition of single trial data from electrode Fz.

RESULTS: In patients with schizophrenia, 40-Hz PLA was significantly reduced (i.e., phase delayed) ($p < .0001$) and was unrelated to reductions in their 40-Hz power or PLF. PLA discriminated patients from healthy control subjects with 85% accuracy compared with 67% for power and 65% for PLF.

CONCLUSIONS: Consistent with the original Kwon *et al.* study, 40-Hz click train–driven gamma oscillations were phase delayed in schizophrenia. Importantly, this phase delay abnormality was substantially larger than the gamma power and phase synchrony abnormalities that have been the focus of prior 40-Hz ASSR studies in schizophrenia. PLA provides a unique neurobiological measure of gamma band abnormalities in schizophrenia, likely reflecting a distinct pathophysiological mechanism from those underlying PLF and power abnormalities.

Keywords: ASSR, Auditory steady-state response, EEG, Gamma, Oscillations, Phase, Schizophrenia

https://doi.org/10.1016/j.bpsc.2018.08.011

Event-related electroencephalography (EEG) signals may be analyzed using time-frequency decomposition methods that separate EEG oscillations into magnitude and phase components for each frequency in EEG, allowing assessment of frequency-specific changes in these signals with respect to task events (1). Among the tasks to which these EEG analysis methods have been applied are so-called steady-state paradigms, in which a stimulus is repeated at a specific frequency to drive EEG oscillations at that frequency. In cases in which an auditory stimulus is repeated at a fixed rate or frequency, the resulting stimulus-driven EEG oscillations are known as the auditory steady-state response (ASSR) (2). Across a wide range of tested frequencies, the ASSR has its peak signal power when an auditory stimulus is presented at a 40-Hz repetition rate, driving 40-Hz gamma frequency oscillations in EEG (2–5). The 40-Hz ASSR has traditionally been quantified by applying a fast Fourier transformation to the time-domain average event-related potential (ERP) to obtain an evoked power measurement in the spectral domain. However, it can be represented in time-frequency space by event-related change in ERP magnitude, known as evoked power; in single trial signal magnitude, known as total power; or by the degree of consistency in signal phase across trial repetitions, known as phase-locking factor (PLF).

Starting with Kwon *et al.* (6), many 40-Hz ASSR studies have shown EEG or magnetoencephalography gamma band evoked power (7–16), total power (5,15,17–22), or PLF (5,9,10,13–17,19,20,22–26) to be reduced in schizophrenia (SZ) [for reviews, see (27,28)], and a recent meta-analysis concluded that these reductions are robust (29). These abnormalities reflect deficits in the amplitude and cross-trial phase coherence of stimulus-driven gamma oscillations in SZ. However, while Kwon *et al.* (6) also reported abnormalities on a measure called phase-delay, which attempted to capture the time between each click onset in a 40-Hz click train and the subsequent negative peak in narrow band filtered time-domain EEG data, this finding was essentially ignored in subsequent 40-Hz ASSR studies. This is the case even though time-frequency decomposition methods provide time-varying measures of the phase angle of oscillations, allowing for comparisons of gamma oscillation phases across diagnostic groups. Therefore, we propose a new measure, the phase-locking angle (PLA), that captures the degree to which a given subject's oscillatory phase leads or lags behind the mean phase angles of stimulus-locked oscillations derived from a reference group such as a sample of healthy control (HC) subjects. Such a measure has not been examined in prior ASSR studies of clinical groups. This may in part be because

ISSN: 2451-9022

commonly used time-frequency analysis software does not return phase angle values by default, limiting the extent to which researchers have been able to understand and exploit the unique insights this information can provide about the temporal characteristics of event-related neuro-oscillations.

Traditional ERP research has focused on characterizing ERP component waveforms by identifying and measuring their peaks. In effect, this approach focuses on either of two specific phase angles of the sinusoidal ERP component waveform—90° (or $\pi/2$ radians) corresponding to the peak of positive-going components such as P1, P300, etc., or 270° (or $-\pi/2$ radians) corresponding to the peak of negative-going components such as N1, N400, etc. These ERP peaks provide evidence of consistent phase, or phase-locking, of specific frequencies of EEG with respect to stimulus onset across trials, as only the oscillations that are phase synchronized across trials survive when trials are averaged to generate an ERP. Similarly, the presence of negative and positive peaks in the grand average ERP waveform derived by averaging ERPs across subjects indicates that the phase of stimulus-evoked oscillations is generally consistent across subjects as well. Through the application of time-frequency analysis, the full range (i.e., 0°–360°) of frequency-specific phase angles can be tracked over time. Examination of time series of phase angles could provide a more comprehensive and refined view of the temporal characteristics of oscillations than has been achieved using traditional ERP peak latency. Such data may inform 40-Hz ASSR analyses by providing a continuous measure of response latency throughout the stimulation period, potentially generating new insights into gamma band dysfunction in SZ.

Changes in EEG magnitude (i.e., power) are typically interpreted as reflecting changes in underlying neuronal activity (i.e., either changes in the local magnitudes of inhibitory and/or excitatory postsynaptic potentials or changes in local synchronization of these potentials). The PLF is generally interpreted as reflecting the consistency of stimulus-evoked phase synchronization of emergent or ongoing (i.e., phase resetting) neuro-oscillatory activity at specific time points across trials. Perhaps because of difficulties associated with its interpretation, the actual mean phase angle across trials is rarely considered except in a few studies. Picton *et al.* (30) used phase information to improve detection of the ASSR, while others have used phase data to directly test for shifts in latency of steady-state visual evoked potentials (31–33).

Using circular statistics, we attempted to replicate and extend the finding of Kwon *et al.* (6) of delayed 40-Hz ASSR in SZ using a novel PLA measure. Specifically, using 40-Hz ASSR EEG data collected from patients with SZ or schizoaffective disorder and age-matched HC subjects, we asked whether 1) SZ patients have delayed PLA in the gamma band response to 40-Hz auditory stimulation relative to HC subjects, in addition to having reduced power and PLF; 2) delayed PLA is specific to the 40-Hz frequency or is also evident in the ASSR evoked by 20-Hz and 30-Hz auditory stimulation; 3) the PLA measures of the ASSR were correlated with evoked/total power or PLF measures; 4) these four measures of different aspects of the 40-Hz ASSR show differential sensitivity to SZ.

METHODS AND MATERIALS

Participants

EEG data from a previously published study (19) of 28 patients with DSM-IV SZ (n = 18) or schizoaffective disorder (n = 10) and 25 HC subjects were analyzed in the present study. The demographic and clinical data for these subjects are summarized in Table 1. All subjects provided written informed consent to participate in this institutional review board–approved study. Additional details regarding participants, experimental paradigm, EEG acquisition, time-frequency analysis, and a basic review of concepts relevant to circular statistics are presented

Table 1. Demographic and Clinical Data for Schizophrenia Patients and Healthy Control Subjects

	Schizophrenia Patients (n = 28)				Healthy Control Subjects (n = 25)			
	Mean	SD	Min	Max	Mean	SD	Min	Max
Age, Years	39.3	10.7	22.1	56.1	36.1	12.5	21.8	59.3
Average Parental SES[a]	33.82	17.4	11	69	33.78	14.7	11	62
Education, Years[b]	13.7	1.7	10	16	16	2.3	12	20
PANSS Positive[c]	15.4	5	7	25				
PANSS Negative	14.3	5.2	7	22				
PANSS General	30.4	9.1	17	54				
Duration of Illness, Years	15.6	9.9	2	36				
Race	22 Caucasian, 5 African American, 1 Asian				16 Caucasian, 4 African American, 3 Hispanic, 2 Asian			
Handedness	27 Right, 1 left				22 Right, 2 left, 1 ambidextrous			
Gender	21 Male, 7 female				14 Male, 11 female			
Diagnosis	16 Paranoid schizophrenia							
	2 Undifferentiated schizophrenia							
	6 Schizoaffective depressed type							
	4 Schizoaffective bipolar type							
Antipsychotic Medication	2 Typical, 20 atypical, 6 both							

Max, maximum; Min, minimum; PANSS, Positive and Negative Syndrome Scale; SES, socioeconomic status.
[a]SES based on the Hollingshead two-factor index (49); higher scores indicate lower SES.
[b]$p < .05$ with independent samples t test.
[c]Ratings not available for 2 patients.

in the Supplement. Figure 1 shows the 40-Hz ASSR ERPs, total power, PLF, and associated mean phase angles within HC and SZ groups at two time points (214 ms and 227 ms) in the middle of the stimulation period.

Statistical Analysis

Evoked power, total power, PLF, and PLA values were extracted from electrode Fz between 200 ms and 400 ms. These values were averaged for power and PLF, but additional steps were required before calculating an average angle value. Owing to the periodic nature of the angle values, averaging over an interval equal to or greater than one complete sine wave cycle (e.g., 25 ms for one 40-Hz cycle) would not be informative because the full period of phase angle measures from each 360° cycle will effectively cancel each other out, leading to an uninterpretable mean angle measure. Therefore, the value of the phase angle at each time point is re-expressed as its difference from the expected angle at that time point. The expected angle is defined as the HC circular mean at a specific time point. This difference defines the PLA, and it is expressed in units of radians (see Supplement). The average PLA at 40 Hz between 200 ms and 400 ms was used for subsequent analysis of the 40-Hz ASSR. Similar PLA calculations were used to capture the 20- and 30-Hz ASSR from 20- and 30-Hz click train blocks as well as the 40-Hz ASSR harmonic generated by 20-Hz stimulation.

PLA univariate analyses were conducted using the Watson-Williams test (34), which is analogous to the one-way analysis of variance in circular statistics. Circular statistics are necessary because the PLA values (radians) are nonlinear and periodic (i.e., not continuous; see Supplement) in their distribution. A significance level of $p = .05$ was used for the Watson-Williams tests.

Before running linear regression and mixed models, all measures (PLA, PLF, and power) were transformed to *z* scores based on the HC mean and SD, using appropriate methods in the case of PLA values (see Supplement). Note that PLF and total power measures were linear, normally distributed, and continuous to begin with, and as such the linear *z* score transformation simply allows all measures to be plotted on the same scale, facilitating comparisons between them. However, the *z* score transformation of PLA values could be considered a nonlinear transformation because it changes periodic values, in radians, to standard units of deviation from the HC group.

Six separate multiple linear regression models were run to examine the pairwise relationships among the four time-frequency measures (evoked/total power, PLF, and PLA) elicited by 40-Hz stimulation. Specifically, using *z* scores, 1) total power was regressed on PLF, 2) PLA was regressed on PLF, 3) PLA was regressed on total power, 4) total power was regressed on evoked power, 5) evoked power was regressed on PLF, and 6) PLA was regressed on evoked power. In each model, a group indicator variable and a group × time-frequency measure interaction term (e.g., group × PLF for models 1, 2, and 5) were included. The interaction term tested for group differences in the regression line slopes. If the interaction term was not significant, it was removed, resulting in a reduced model that tested the relationship between the time-frequency measures assuming a common slope across groups. Diagnostic plots were used to assess model assumptions of normality of residuals and homogeneity of variances. Bonferroni correction was used ($p = .05/6$ or .00834) for these regression tests.

To assess possible differential sensitivity to the pathophysiology of SZ, 40-Hz PLA, evoked/total power, and PLF *z* scores were tested in a mixed model with group as the

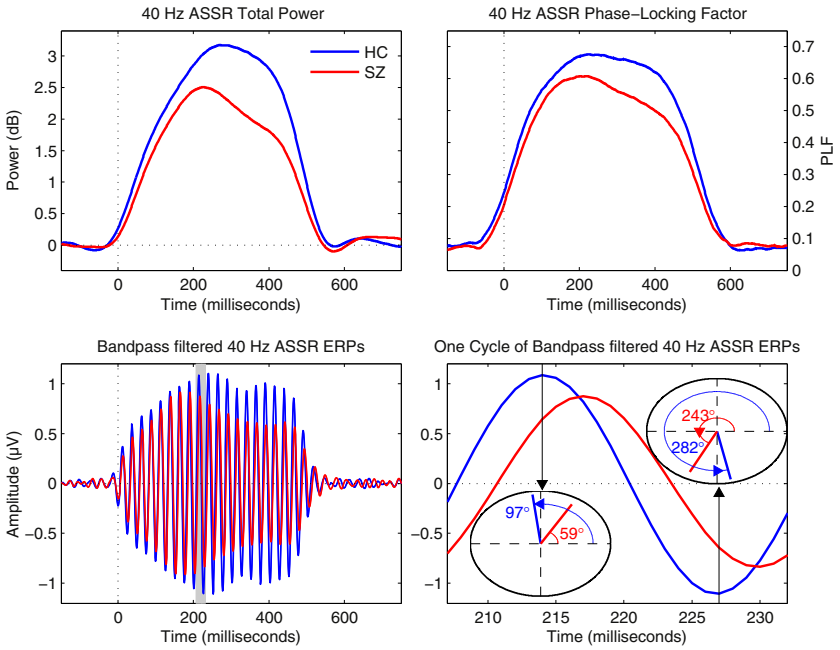

Figure 1. Group differences in total power (top left panel) and phase-locking factor (PLF) (top right panel) group averages for the 40-Hz auditory steady-state response (ASSR) are plotted. The 30- to 50-Hz bandpass filtered 40-Hz ASSR electroencephalography data are overlaid for the healthy control (HC; blue) group and the schizophrenia (SZ; red) group on the bottom left. Data in the gray highlighted area (bottom left panel) are magnified (bottom right panel) to show group differences in the mean phase angles on the unit circle at 214 ms (inset lower left circle) and 227 ms (inset upper right circle), approximately corresponding to the HC group event-related potential (ERP) peak and trough. These points differ by approximately 13 ms, or half a 40-Hz sine wave cycle. The mean phase angles of the SZ group at these time points indicate that the phase of their 40-Hz click train–driven gamma band oscillation lags behind the HC group by approximately 38° (3 ms; phase lags indicated by red, relative to blue, mean phase angle vectors).

between-subjects fixed factor and time-frequency measure *z* score (PLA, evoked power, total power, PLF) as the within-subjects fixed factor. Subject nested within group was a random factor, and the main effects, interaction, and follow-up contrasts were estimated with an unstructured covariance matrix using PROC MIXED in SAS 9.4 (SAS Institute Inc., Cary, NC). A similar model assessing the frequency specificity of potential PLA abnormalities in SZ included steady-state frequency (20 Hz, 30 Hz, 40 Hz) as a within-subjects fixed factor. Given our previously reported significant 40-Hz total power and PLF deficits in the SZ group relative to HC group (19) as well as the planned group comparisons of PLA using Watson-Williams tests described above, significant group × within-subject factor interactions in the mixed models were followed up with tests of relative differences, comparing the groups on three orthogonal Helmert contrasts between the measures. In the first model, these contrasts were 1) evoked minus total power, 2) PLF minus the mean of evoked and total power, and 3) PLA minus the mean of the other measures. In the second model, these contrasts were 1) 20-Hz frequency minus 30-Hz frequency, and 2) 40-Hz frequency minus the mean of 20- and 30-Hz frequency. To examine relationships between clinical symptoms and PLA measures in the SZ group, we conducted Pearson correlations between Positive and Negative Syndrome Scale (35) positive, negative, general, and total symptom subscale scores and 40-Hz PLA *z* scores.

RESULTS

Visual inspection of box plots of the *z*-scored data revealed one SZ outlier on the 40-Hz PLA measure (PLA *z* score >6 SD from HC mean). There were no clear problems or issues with this patient's EEG recording or single trial data. His 40-Hz PLA data were removed from the 40-Hz PLA Watson-Williams test, censored with an indicator variable in regression tests, or omitted from the mixed models that can account for missing data.

Watson-Williams Tests (One-Way Analysis of Variance)

There was a significant group difference in the 40-Hz PLA (Figure 2), with SZ patients showing lagged PLA relative to HC subjects ($F_{1,50}$ = 27.51, $p < .0001$). Tests of the PLA in other

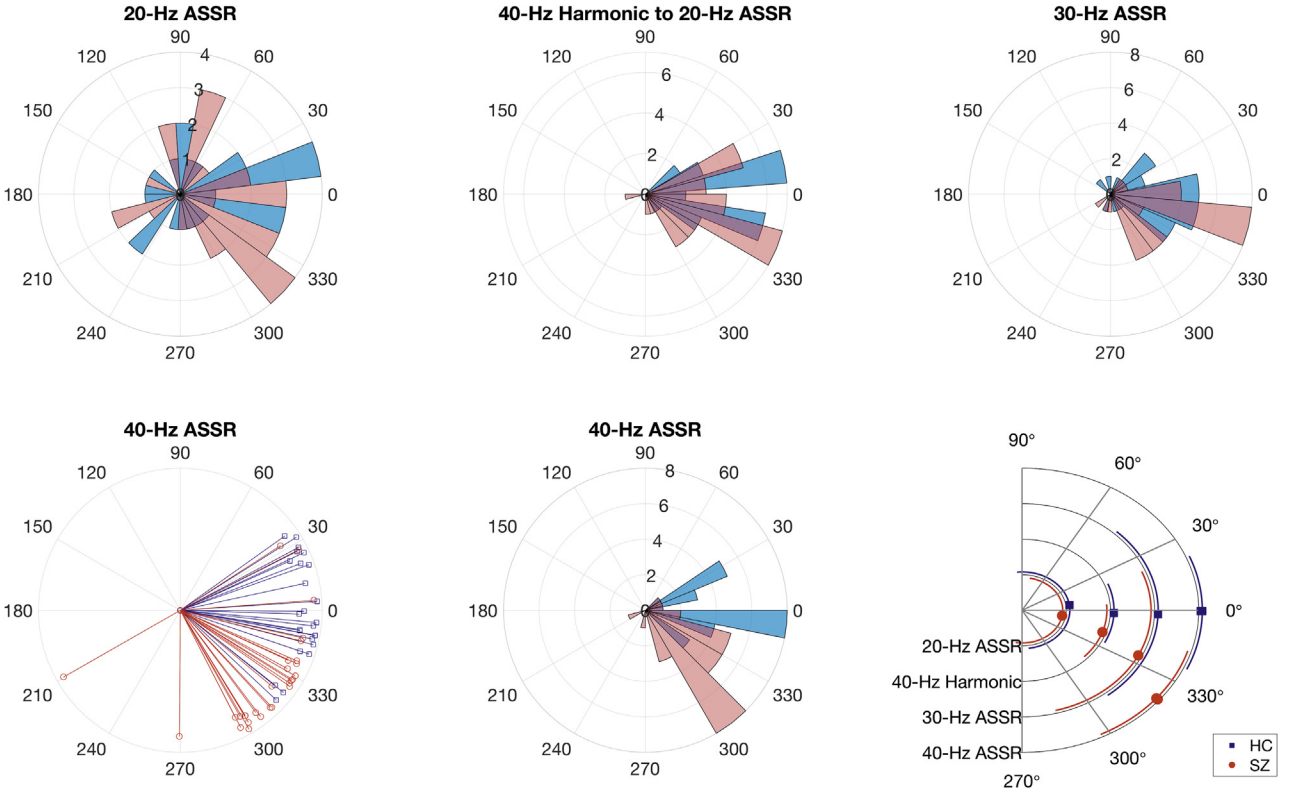

Figure 2. Polar histogram overlays depict the distribution of phase-locking angle (PLA) measures in healthy control (HC, blue) and schizophrenia (SZ, red) groups in the 20-Hz condition (top left panel), 40-Hz harmonic during 20-Hz stimulation (top center panel), 30-Hz condition (top right panel), and 40-Hz stimulation condition (bottom center panel). On these histograms, each wedge represents a phase angle bin, and its length indicates the number of subjects who fall into that bin. Single-subject PLA vectors are plotted for the 40-Hz condition in the bottom left panel, with each blue line representing one HC subject and each red line representing one SZ patient. In the bottom right panel, all PLA group average values (HC group: blue squares; SZ group: red circles) ± associated SDs (depicted by colored arcs centered on each PLA group mean) are plotted for each auditory steady-state response (ASSR) condition (black semicircle lines) labeled along the y axis. The plot in the bottom right panel shows that the phase angle lag in the SZ group relative to HC group is greater for the 40-Hz ASSR condition than for the other ASSR conditions, including the 40-Hz harmonic elicited during 20-Hz stimulation.

steady-state blocks revealed no difference at 20 Hz ($F_{1,51}$ = 0.4744, p = .4941), marginal reductions in SZ patients at 30 Hz ($F_{1,51}$ = 3.71, p = .0599), and marginal reductions in SZ patients in the 40-Hz harmonic response during the 20-Hz click train block ($F_{1,51}$ = 3.91, p = .0534).

Linear Regression Models

The pairwise relationships among the four 40-Hz time-frequency measures are plotted in Figure 3. There were no significant slope differences between groups in any of these relationships (all p values $>$ .07). Total power and PLF z scores showed a significant direct relationship. The reduced model testing the common slope of the regression line predicting total power from PLF showed a strong positive linear relationship between the two measures, but model diagnostic plots suggested a quadratic term should be added. The final model (Table 2) revealed a strong quadratic relationship between PLF and total power in both groups, with the steep direct association starting to flatten out at the lower levels of PLF. In the models regressing PLA on PLF and total power, reduced models showed no evidence of a significant association between PLA and either PLF or total power. Group differences in PLA remained significant after controlling for either PLF or total power (Table 2). Evoked and total power z scores showed a significant relationship, although the evoked power data were highly skewed. Similar to total power, evoked power appeared to show a nonlinear relationship with PLF, and a quadratic PLF term was added to this model. The final model indicated both linear and marginal quadratic PLF relationships with evoked power that did not differ between the groups. Finally, there was no evidence of a relationship between evoked power and PLA.

Mixed Models

In the 40-Hz mixed model that included all four z-scored time-frequency measures, there was a significant group $\times$ time-frequency measure interaction ($F_{3,51}$ = 4.81, p = .005). Helmert follow-up contrasts revealed that the group difference in evoked and total power were statistically equivalent (t_{51} = −0.97, p = .3347), as was the difference in PLF and the average of these two power measures (t_{51} = 1.15, p = .2563). Importantly, the group difference in 40-Hz PLA was significantly greater than the average group difference in evoked power, total power, and PLF (t_{51} = 3.25, p = .002). This approximately 1 SD (1.113 $\pm$ 0.343) increased abnormality in the PLA measure can be appreciated in Figure 4. Figure 5 displays the receiver operating characteristic curve for each measure and represents the strength of the discrimination between SZ patients and HC subjects using the area under the curve statistic.

In the mixed model analysis of PLA z scores that included steady-state frequency (20 Hz, 30 Hz, 40 Hz) from the corresponding click train block, there was a significant group $\times$ steady-state frequency interaction ($F_{2,51}$ = 6.64, p = .0027). Helmert contrasts revealed that the group difference in 20-Hz and 30-Hz PLA was statistically equivalent (t_{51} = −0.89, p = .3774), but the group difference in 40-Hz PLA was significantly greater than the average group difference in 20- and 30-Hz PLA (t_{51} = 3.65, p = .0006) (Figure 4, right). A separate analysis of data from electrode Cz produced a similar pattern of results.

Clinical Correlations

There were no symptom correlations with 40-Hz PLA z scores (all p values $>$ .32). The 40-Hz PLA effect was not influenced

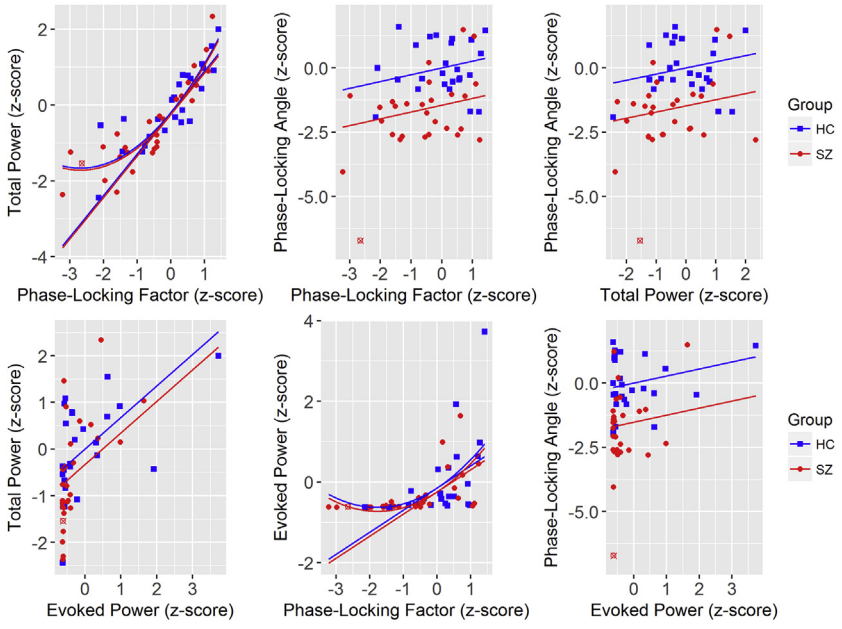

Figure 3. The relationship between three 40-Hz time-frequency measures is shown with separate scatterplots for total power vs. phase-locking factor (PLF) (upper left panel), phase-locking angle (PLA) vs. PLF (upper middle panel), PLA vs. total power (upper right panel), total power vs. evoked power (lower left panel), evoked power vs. PLF (lower middle panel), and PLA vs. evoked power (lower right panel). Each point represents single subject data (healthy control [HC] subjects: blue squares; schizophrenia [SZ] patients: red circles), averaged across 200–400 ms at the 40-Hz electroencephalography frequency in response to the 40-Hz click train. Each measure is z-scored relative to the mean and SD of the HC group. Separate regression lines are plotted for each group (SZ group: red; HC group: blue), but slopes are the same because group differences in slopes were not significant. For evoked and total power vs. PLF, both linear and quadratic regression line fits are shown, with quadratic fit significantly increasing the variance accounted for over and above the linear fit. The linear and quadratic PLF variables accounted for approximately 76% of the variance in total power and 31% of the variance in evoked power, controlling for group (total power R^2 change = .7618; evoked power R^2 change = .3086). PLA was not significantly related to PLF (upper middle panel), total power (upper right panel), or evoked power (lower right panel). One SZ patient with extremely small PLA values was censored from regressions but plotted as an open red circle marked by an X for reference.

Table 2. Relationships Between 40-Hz Time-Frequency Measure *z* Scores

Model	Effect	β	SE	*t*	*p* Value
Total Power vs. PLF	Intercept	−.198	0.105	−1.892	.0644
	Group	−.052	0.137	−0.379	.7065
	PLF	1.092	0.084	12.992	< .0001
	PLF^2	.207	0.044	4.649	< .0001
PLA vs. PLF	Intercept	−.003	0.222	−0.014	.989
	Group	−1.451	0.318	−4.560	< .0001
	PLF	.265	0.141	1.875	.0667
PLA vs. Total Power	Intercept	−.003	0.223	−0.014	.989
	Group	−1.477	0.319	−4.624	< .0001
	Total power	.240	0.146	1.646	.106
Evoked Power vs. Total Power	Intercept	4×10^{-10}	0.140	0.000	1.000
	Group	−.099	0.201	−0.496	.6218
	Total power	3.688	0.091	4.033	.0002
Evoked Power vs. PLF	Intercept	−.149	0.148	−1.002	.3213
	Group	−.098	0.194	−0.504	.6164
	PLF	.547	0.118	4.625	< .0001
	PLF^2	.155	0.064	2.405	.0201
PLA vs. Evoked Power	Intercept	−.003	0.225	−0.014	.989
	Group	−1.523	0.318	−4.792	< .0001
	Evoked power	.274	0.198	1.381	.174

PLA, phase-locking angle; PLF, phase-locking factor.

by the SZ (n = 17) versus schizoaffective disorder (n = 10) distinction; both subgroups showed significant and similar phase delays relative to the HC group.

DISCUSSION

This study compared EEG time-frequency measures of the 40-Hz ASSR between SZ patients and HC subjects with a focus on the PLA, a time point–specific estimate of the difference from the HC group average in mean phase angle across single trials, and yielded three major findings. First, when averaged over the 200- to 400-ms post–click train–onset time window during which stimulus-driven oscillations achieve steady state, the 40-Hz PLA was significantly delayed in SZ patients relative to HC subjects. Second, the 40-Hz PLA measure showed no substantial relationship with 40-Hz power or PLF in SZ patients or HC subjects. Third, the 40-Hz PLA phase delay in SZ patients was significantly greater than 40-Hz power and PLF deficits. Given every possible permutation of HC-SZ pairs in the sample, the area under the curve represents the percentage of pairs where the HC subject's value is greater than the SZ patient's value. In the case of 40-Hz PLA, the SZ patient's oscillation phase lagged behind the HC subject's oscillation phase in approximately 85% of the combinations. By contrast, the SZ patient had reduced 40-Hz evoked power, total power, or PLF values compared with the HC subject in only approximately 62%, approximately 65%, and approximately 67% of the combinations.

In their seminal study, Kwon *et al.* (6) also reported a delay in the 40-Hz ASSR in SZ. However, no subsequent ASSR studies attempted to replicate this finding. The current study not only replicated the basic 40-Hz phase-delay finding using a more comprehensive analytic approach, but also demonstrated that the phase delay exhibited by SZ patients was specific to 40-Hz oscillations. In a repeated-measures analysis of the PLA measure from three different steady-state stimulation frequencies, phase delay in SZ patients was significantly greater at 40 Hz relative to both 30 Hz and 20 Hz, neither of which showed abnormal PLA. The 40-Hz harmonic in the EEG response to 20-Hz stimulation was marginally delayed in SZ patients relative to HC subjects. Accordingly, our findings provide new evidence of specific gamma oscillation phase delay abnormalities during 40-Hz auditory steady-state stimulation in SZ.

Kwon *et al.* (6) demonstrated 40-Hz phase delays in SZ using peak picking methods. Specifically, the latency of each gamma oscillation peak was measured relative to the preceding click, with subsequent analysis of these latency measures. Time-frequency analysis toolboxes typically provide frequency-specific and time point–specific measures of power and phase synchrony from event-related EEG data. However, such software generally does not include methods to analyze the mean phase angles, likely contributing to the absence of attempts to replicate the finding of Kwon *et al.* of 40-Hz phase delay in SZ. In this study, we implemented such a method, which involved extracting the mean phase angle across trials after time-frequency decomposition. One approach to analyzing these data is to use circular statistics to compare groups on the phase angles from 40-Hz oscillations. As can be seen in the Supplemental Video (see also at https://www.youtube.com/watch?v=OHWkclMn3Vo), the angle measures show excellent correspondence to the ASSR ERP in that peaks in the grand average ERP occur when the angle is 90°, and troughs occur when the angle is 270°. However, our approach uses the PLA estimates at every sample in the epoch to track the phase over time, rather than limiting analysis to the peaks or troughs of the oscillation cycle. Furthermore, by

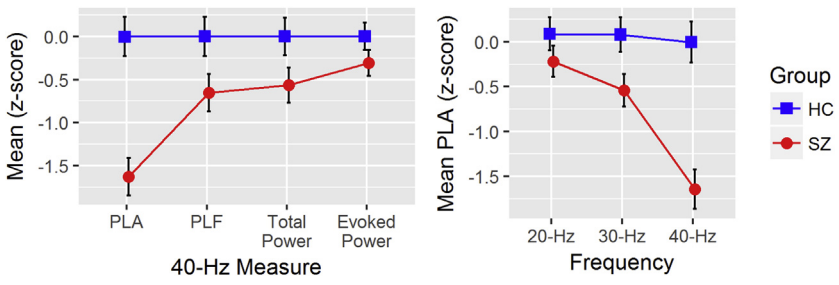

Figure 4. Group differences in the four 40-Hz time-frequency measures are plotted in the left panel. Because each measure is *z*-scored to the healthy control (HC: blue squares) group, HC group average values are equal to zero, and the schizophrenia (SZ: red circles) group negative average values indicate lagged or reduced responses for phase-locking angle (PLA), phase-locking factor (PLF), total power, and evoked power measures. Group differences in the 20-, 30-, and 40-Hz PLA responses from the corresponding steady-state stimulation frequency trials are plotted in the right panel. Each measure is *z*-scored to the HC group; the 40-Hz PLA data are identical in both panels but are plotted twice for reference.

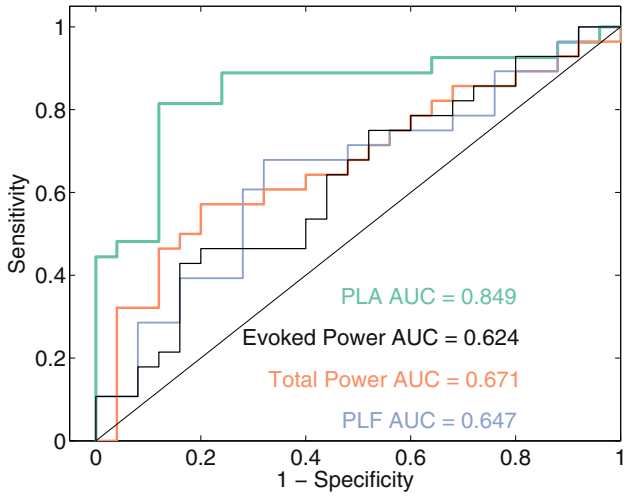

Figure 5. The 40-Hz phase-locking angle (PLA), evoked power, total power, and phase-locking factor (PLF) receiver operating characteristic curves are plotted to show the differential performance of each measure as a classifier discriminating between patients with schizophrenia and healthy control subjects. Each measure's corresponding area under the curve (AUC) value quantifies the discriminative strength of each classifier. PLA, evoked power, total power, and PLF *z* scores classified patients with schizophrenia and healthy control subjects with 84.9%, 62.4%, 67.1%, and 64.7% accuracy.

standardizing PLA measures relative to HC, we eliminated the need to use circular statistics, allowing PLA to be combined with or compared with other linear measures in multivariate analyses.

One patient exhibited extreme delay in 40-Hz PLA during 40-Hz stimulation. Whereas this patient had reduced 40-Hz PLF, power, and 30-Hz PLA measures relative to the group average, he was not an outlier on any of those measures or on any clinical and/or demographic variables. This suggests that this patient was unable to produce a 40-Hz ASSR and further suggests that PLA can be a useful tool for assessing ASSR data quality, consistent with its use in a previous study (30). Therefore, PLA-like measures may prove useful for screening single-subject ASSR data quality, supplementing artifact rejection and inspection techniques employed in electrophysiological research.

The 40-Hz ASSR PLA better discriminated SZ patients from HC subjects than power or PLF, suggesting the relatively greater potential utility of PLA as an illness biomarker. However, it is important to note that the 40-Hz phase delay in SZ was not uniform over time. Whereas a statistically significant difference in the 40-Hz PLA was evident 25 ms after stimulus onset and was present throughout the stimulation period, it was particularly pronounced between 170 ms and 350 ms after onset (Figure 6). This suggests that midtrain 40-Hz ASSR stimulation may be particularly effective for detecting gamma phase delays in SZ, perhaps owing to recurrent driving of the auditory cortex at the gamma frequency. Nonetheless, marginally significant gamma band phase delays were also evident in response to 30-Hz stimulation and the 40-Hz harmonic response to 20-Hz stimulation. Thus, the pathophysiological mechanism underlying phase delayed gamma oscillations in SZ patients may be evident with varying sensitivity across a variety of task conditions and stimuli that elicit gamma oscillations.

As the average 40-Hz phase lag in SZ patients was 38° or approximately 3 ms relative to HC, any candidate pathophysiological mechanism underlying this effect must operate on a similar time scale. At the cellular level, fast-spiking parvalbumin expressing gamma-aminobutyric acidergic basket cells generate gamma oscillations (36,37). In the boutons of such basket cells in auditory cortex, Moyer *et al.* (38) observed decreased glutamic acid decarboxylase 65, a protein involved in gamma-aminobutyric acid synthesis, postmortem in SZ patients relative to HC subjects. This complements similar postmortem findings of reduced glutamic acid decarboxylase 67 expression in other brain regions, including prefrontal cortex (39). In the auditory cortex, this glutamic acid decarboxylase 65 reduction could lead to inefficient gamma-aminobutyric acidergic transmission and the delayed gamma oscillations observed in the 40-Hz ASSR.

N-methyl-D-aspartate receptor hypofunction has been implicated in the pathophysiology of SZ (40,41). *N*-methyl-D-aspartate receptor dysfunction on parvalbumin interneurons has been proposed as one possible source of gamma oscillation abnormalities in SZ (42), but this primary role has been questioned (43,44). This ongoing debate may be informed by analysis of a measure such as PLA in various animal models and pharmacological challenge studies because PLA may be more sensitive than power or PLF measures to the gamma oscillation abnormalities in SZ.

All patients in this study were taking typical and/or atypical types of antipsychotic medication. This medication confound

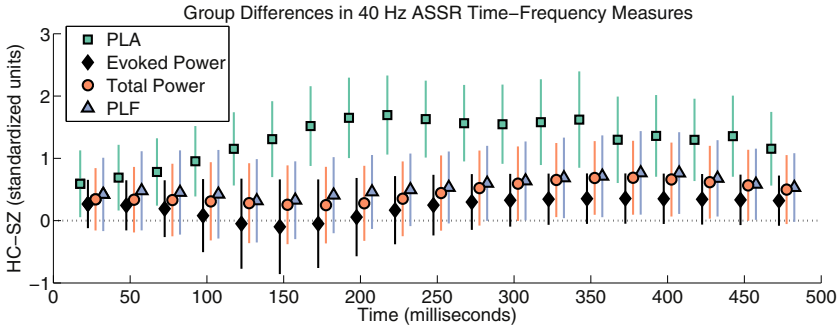

Figure 6. Healthy control (HC) group minus schizophrenia (SZ) group differences from electrode Fz for phase-locking angle (PLA; square), evoked power (diamond), total power (circle), and phase-locking factor (PLF; triangle) are plotted at each 25-ms time point throughout the steady-state stimulation period. Differences are in standardized units relative to the HC mean and SD for each measure, allowing the group differences in the measures to be compared despite their measurement scale differences. The lines represent 95% confidence intervals for the independent samples *t* test differences. The horizontal dotted black line reflects no group difference. ASSR, auditory steady-state response.

has been present in all prior 40-Hz ASSR SZ studies, and in one study, patients taking atypical antipsychotics (clozapine, olanzapine, and risperidone) had greater 40-Hz power than HC subjects (45). Nine patients were also taking benzodiazepines, which did not appear to affect any of the measures (see Supplement). Studies of unmedicated individuals who are at high risk for psychosis may at least partially address the potential confounds of medications.

While both *N*-methyl-D-aspartate receptor hypofunction and impaired gamma-aminobutyric acidergic neurotransmission have been implicated in the pathophysiology of gamma oscillation abnormalities in SZ, this noninvasive EEG study cannot directly address the source of 40-Hz ASSR abnormalities at the cellular level. Accordingly, determining the pathophysiological significance of delayed PLA requires additional animal studies focused on elucidating the mechanisms underlying the onset and phase regularity of stimulus-evoked gamma oscillations.

In addition to cellular abnormalities at the microcircuit level that may contribute to phase-delayed gamma oscillations in SZ, effects of attention and task parameters must be considered. There were no explicit behavioral measurements in the task, and while all subjects were told to remain alert and attentive, it is possible that HC subjects attended to the stimuli better than SZ patients. Attention has previously been shown to enhance the 40-Hz ASSR (46). Additional studies are required to tease apart effects of attention and other task parameters.

We did not observe significant clinical symptom correlations with the PLA in our SZ sample. Many factors, including insufficient power, medication, symptom instability, and measurement error associated with symptom ratings, can make the discovery of such correlations challenging (47,48). Larger-sample 40-Hz ASSR studies in SZ should incorporate PLA to assess its clinical correlations as well as its cognitive, pharmacological, and genetic correlates.

In conclusion, while reductions in power and phase synchrony of ASSR-evoked gamma oscillations have been consistently reported in SZ, the current study suggests that these oscillations are also delayed in SZ. Importantly, this phase delay abnormality has a larger pathophysiological effect size than either the reductions in gamma power or PLF. Moreover, the gamma band–specific PLA abnormality in SZ is unrelated to their power and PLF deficits, suggesting that it may be subserved by a distinct pathophysiological mechanism. More research is needed to fully elucidate the meaning of the 40-Hz PLA abnormality in SZ identified here.

ACKNOWLEDGMENTS AND DISCLOSURES

This study was funded by the National Institute of Mental Health (Grant No. R01MH058262 [to JMF]) and the Department of Veterans Affairs (Senior Research Career Scientist award [to JMF]; I01 CX0004971 [to JMF]).

DHM is a consultant for Boehringer Ingelheim, Alkermes, and Takeda. The other authors report no biomedical financial interests or potential conflicts of interest.

ARTICLE INFORMATION

From the Mental Health Service (BJR, JMF, DHM), San Francisco Veterans Affairs Health Care System; Northern California Institute for Research and Education (BJR), San Francisco Veterans Affairs Medical Center; and Department of Psychiatry (JMF, DHM), University of California, San Francisco, San Francisco, California.

Address correspondence to Daniel H. Mathalon, Ph.D., M.D., Mental Health Service 116D, San Francisco Veterans Affairs Health Care System, 4150 Clement Street, San Francisco CA, 94121; E-mail: daniel.mathalon@ucsf.edu.

Received Jul 26, 2018; revised and accepted Aug 15, 2018.

Supplementary material cited in this article is available online at https://doi.org/10.1016/j.bpsc.2018.08.011.

REFERENCES

1. Mathalon DH, Sohal VS (2015): Neural oscillations and synchrony in brain dysfunction and neuropsychiatric disorders: It's about time. JAMA Psychiatry 72:840–844.
2. Galambos R, Makeig S, Talmachoff PJ (1981): A 40-Hz auditory potential recorded from the human scalp. Proc Natl Acad Sci U S A 78:2643–2647.
3. Pastor MA, Artieda J, Arbizu J, Marti-Climent JM, Penuelas I, Masdeu JC (2002): Activation of human cerebral and cerebellar cortex by auditory stimulation at 40 Hz. J Neurosci 22:10501–10506.
4. O'Donnell BF, Hetrick WP, Vohs JL, Krishnan GP, Carroll CA, Shekhar A (2004): Neural synchronization deficits to auditory stimulation in bipolar disorder. Neuroreport 15:1369–1372.
5. Krishnan GP, Hetrick WP, Brenner CA, Shekhar A, Steffen AN, O'Donnell BF (2009): Steady state and induced auditory gamma deficits in schizophrenia. Neuroimage 47:1711–1719.
6. Kwon JS, O'Donnell BF, Wallenstein GV, Greene RW, Hirayasu Y, Nestor PG, *et al.* (1999): Gamma frequency-range abnormalities to auditory stimulation in schizophrenia. Arch Gen Psychiatry 56:1001–1005.
7. Brenner CA, Sporns O, Lysaker PH, O'Donnell BF (2003): EEG synchronization to modulated auditory tones in schizophrenia, schizoaffective disorder, and schizotypal personality disorder. Am J Psychiatry 160:2238–2240.
8. Vierling-Claassen D, Siekmeier P, Stufflebeam S, Kopell N (2008): Modeling GABA alterations in schizophrenia: A link between impaired inhibition and altered gamma and beta range auditory entrainment. J Neurophysiol 99:2656–2671.
9. Spencer KM, Niznikiewicz MA, Nestor PG, Shenton ME, McCarley RW (2009): Left auditory cortex gamma synchronization and auditory hallucination symptoms in schizophrenia. BMC Neurosci 10:85.
10. Light GA, Hsu JL, Hsieh MH, Meyer-Gomes K, Sprock J, Swerdlow NR, *et al.* (2006): Gamma band oscillations reveal neural network cortical coherence dysfunction in schizophrenia patients. Biol Psychiatry 60:1231–1240.
11. Komek K, Bard Ermentrout G, Walker CP, Cho RY (2012): Dopamine and gamma band synchrony in schizophrenia—insights from computational and empirical studies. Eur J Neurosci 36:2146–2155.
12. Hamm JP, Bobilev AM, Hayrynen LK, Hudgens-Haney ME, Oliver WT, Parker DA, *et al.* (2015): Stimulus train duration but not attention moderates gamma-band entrainment abnormalities in schizophrenia. Schizophr Res 165:97–102.
13. Teale P, Collins D, Maharajh K, Rojas DC, Kronberg E, Reite M (2008): Cortical source estimates of gamma band amplitude and phase are different in schizophrenia. Neuroimage 42:1481–1489.
14. Light GA, Zhang W, Joshi YB, Bhakta S, Talledo JA, Swerdlow NR (2017): Single-dose memantine improves cortical oscillatory response dynamics in patients with schizophrenia. Neuropsychopharmacology 42:2633–2639.
15. Griskova-Bulanova I, Dapsys K, Melynyte S, Voicikas A, Maciulis V, Andruskevicius S, *et al.* (2018): 40Hz auditory steady-state response in schizophrenia: Sensitivity to stimulation type (clicks versus flutter amplitude-modulated tones). Neurosci Lett 662:152–157.
16. Zhou TH, Mueller NE, Spencer KM, Mallya SG, Lewandowski KE, Norris LA, *et al.* (2018): Auditory steady state response deficits are associated with symptom severity and poor functioning in patients with psychotic disorder. Schizophr Res 201:278–286.

17. Tada M, Nagai T, Kirihara K, Koike S, Suga M, Araki T, *et al.* (2016): Differential alterations of auditory gamma oscillatory responses between pre-onset high-risk individuals and first-episode schizophrenia. Cereb Cortex 26:1027–1035.
18. Wilson TW, Hernandez OO, Asherin RM, Teale PD, Reite ML, Rojas DC (2008): Cortical gamma generators suggest abnormal auditory circuitry in early-onset psychosis. Cereb Cortex 18:371–378.
19. Roach BJ, Ford JM, Hoffman RE, Mathalon DH (2013): Converging evidence for gamma synchrony deficits in schizophrenia. Suppl Clin Neurophysiol 62:163–180.
20. Edgar JC, Chen YH, Lanza M, Howell B, Chow VY, Heiken K, *et al.* (2014): Cortical thickness as a contributor to abnormal oscillations in schizophrenia? Neuroimage Clin 4:122–129.
21. Tsuchimoto R, Kanba S, Hirano S, Oribe N, Ueno T, Hirano Y, *et al.* (2011): Reduced high and low frequency gamma synchronization in patients with chronic schizophrenia. Schizophr Res 133:99–105.
22. Wang J, Tang Y, Curtin A, Chan RCK, Wang Y, Li H, *et al.* (2018): Abnormal auditory-evoked gamma band oscillations in first-episode schizophrenia during both eye open and eye close states. Prog Neuropsychopharmacol Biol Psychiatry 86:279–286.
23. Spencer KM, Salisbury DF, Shenton ME, McCarley RW (2008): Gamma-band auditory steady-state responses are impaired in first episode psychosis. Biol Psychiatry 64:369–375.
24. Hirano Y, Oribe N, Kanba S, Onitsuka T, Nestor PG, Spencer KM (2015): Spontaneous gamma activity in schizophrenia. JAMA Psychiatry 72:813–821.
25. Kirihara K, Rissling AJ, Swerdlow NR, Braff DL, Light GA (2012): Hierarchical organization of gamma and theta oscillatory dynamics in schizophrenia. Biol Psychiatry 71:873–880.
26. Puvvada KC, Summerfelt A, Du X, Krishna N, Kochunov P, Rowland LM, *et al.* (2018): Delta vs gamma auditory steady state synchrony in schizophrenia. Schizophr Bull 44:378–387.
27. Brenner CA, Krishnan GP, Vohs JL, Ahn WY, Hetrick WP, Morzorati SL, *et al.* (2009): Steady state responses: Electrophysiological assessment of sensory function in schizophrenia. Schizophr Bull 35:1065–1077.
28. O'Donnell BF, Vohs JL, Krishnan GP, Rass O, Hetrick WP, Morzorati SL (2013): The auditory steady-state response (ASSR): A translational biomarker for schizophrenia. Suppl Clin Neurophysiol 62:101–112.
29. Thune H, Recasens M, Uhlhaas PJ (2016): The 40-Hz auditory steady-state response in patients with schizophrenia: A meta-analysis. JAMA Psychiatry 73:1145–1153.
30. Picton TW, Dimitrijevic A, John MS, Van Roon P (2001): The use of phase in the detection of auditory steady-state responses. Clin Neurophysiol 112:1698–1711.
31. Wang J, Wade AR (2011): Differential attentional modulation of cortical responses to S-cone and luminance stimuli. J Vis 11:1.
32. Di Russo F, Spinelli D (2002): Effects of sustained, voluntary attention on amplitude and latency of steady-state visual evoked potential: A costs and benefits analysis. Clin Neurophysiol 113:1771–1777.
33. Di Russo F, Spinelli D (1999): Spatial attention has different effects on the magno- and parvocellular pathways. Neuroreport 10:2755–2762.
34. Hollingshead AB, Redlich FC (1958): Social Class and Mental Illness: Community Study. Hoboken, NJ: John Wiley & Sons Inc.
35. Watson GS, Williams EJ (1956): On the construction of significance tests on the circle and the sphere. Biometrika 43:344–352.
36. Kay SR, Fiszbein A, Opler LA (1987): The positive and negative syndrome scale (PANSS) for schizophrenia. Schizophr Bull 13:261–276.
37. Sohal VS, Zhang F, Yizhar O, Deisseroth K (2009): Parvalbumin neurons and gamma rhythms enhance cortical circuit performance. Nature 459:698–702.
38. Cardin JA, Carlen M, Meletis K, Knoblich U, Zhang F, Deisseroth K, *et al.* (2009): Driving fast-spiking cells induces gamma rhythm and controls sensory responses. Nature 459:663–667.
39. Moyer CE, Delevich KM, Fish KN, Asafu-Adjei JK, Sampson AR, Dorph-Petersen KA, *et al.* (2012): Reduced glutamate decarboxylase 65 protein within primary auditory cortex inhibitory boutons in schizophrenia. Biol Psychiatry 72:734–743.
40. Rocco BR, Lewis DA, Fish KN (2016): Markedly lower glutamic acid decarboxylase 67 protein levels in a subset of boutons in schizophrenia. Biol Psychiatry 79:1006–1015.
41. Krystal JH, Anand A, Moghaddam B (2002): Effects of NMDA receptor antagonists: Implications for the pathophysiology of schizophrenia. Arch Gen Psychiatry 59:663–664.
42. Coyle JT, Tsai G, Goff D (2003): Converging evidence of NMDA receptor hypofunction in the pathophysiology of schizophrenia. Ann N Y Acad Sci 1003:318–327.
43. Nakazawa K, Zsiros V, Jiang Z, Nakao K, Kolata S, Zhang S, *et al.* (2012): GABAergic interneuron origin of schizophrenia pathophysiology. Neuropharmacology 62:1574–1583.
44. Gonzalez-Burgos G, Lewis DA (2012): NMDA receptor hypofunction, parvalbumin-positive neurons, and cortical gamma oscillations in schizophrenia. Schizophr Bull 38:950–957.
45. Rotaru DC, Lewis DA, Gonzalez-Burgos G (2012): The role of glutamatergic inputs onto parvalbumin-positive interneurons: Relevance for schizophrenia. Rev Neurosci 23:97–109.
46. Hong LE, Summerfelt A, McMahon R, Adami H, Francis G, Elliott A, *et al.* (2004): Evoked gamma band synchronization and the liability for schizophrenia. Schizophr Res 70:293–302.
47. Skosnik PD, Krishnan GP, O'Donnell BF (2007): The effect of selective attention on the gamma-band auditory steady-state response. Neurosci Lett 420:223–228.
48. Mathalon DH, Ford JM (2012): Neurobiology of schizophrenia: Search for the elusive correlation with symptoms. Front Hum Neurosci 6:136.
49. Ford JM (2018): The difficulty in finding relationships between ERPs and clinical symptoms of schizophrenia. Clin EEG Neurosci 49:6–7.